Strategies for improving electrical transport of vanadium and molybdenum oxide nanowire electrodes

Yuqiang Pi[a], Chunhua Han[a], Liqiang Mai[a,b,*], Lin Xu[a], Xu Xu[a], Bin Hu[a]

[a] State Key Laboratory of Advanced Technology for Materials Synthesis and Processing,
WUT-Harvard Joint Nano Key Laboratory, Wuhan University of Technology, Wuhan, 430070, China
[b] Department of Chemistry and Chemical Biology, Harvard University, Cambridge, Massachusetts 02138, USA

Abstract

Li-ion battery for portable electronic devices and hybrid electric vehicles has gained great importance for energy storage today. However, there still exists an important issue in Li-ion battery, which is the capacity fading with cycling that largely limits the electrochemical performance and commercialization. Because of the existence of the specific layered structure of vanadium and molybdenum oxides, it is relatively easy to improve the conductivity by introducing high conductivity substance into the structure or coating them on the material surface, such as metallic ion, conductive polymer and so on. This review mainly focuses on some improvement strategies in vanadium and molybdenum oxide nanowire electrodes resulting in enhanced electrical transport and thus better electrochemical performances.

Keywords: Conductivity; Vanadium and molybdenum oxides; Doping; Coating; Prelithiation

1. Introduction

Battery as energy storage device has been widely applied in different fields. A battery mainly consists of three parts, anode, cathode and electrolyte, aiming to realize the conversion between chemical potential and electrical energy. In these years, layered oxide cathode materials have attracted much attention for fundamental investigation and commercialization [1]. The layered oxides of vanadium and molybdenum have long been defined as promising cathode materials with the high theoretical capacity and potential application of commercialization [1-8]. However, capacity fading and unsatisfactory cycling stability limit the development and applications of these electrode materials, due to the kinetic limitations for deep discharge and limited diffusion of lithium ion in the solid state. Our group has designed a single nanowire electrochemical device as a unique platform for in-situ probing the intrinsic reason for electrode capacity fading in Li-ion based energy storage devices [9]. Based on this device, a conclusion can be drawn that conductivity of the nanowire electrode decreases reversibly or not during the electrochemical process, which limits its cycling stability. Therefore, how to restrain the conductivity decrease of electrode materials becomes a key issue for improving the performance of lithium ion batteries. To date, there have been few reviews which systematically summarized the optimization strategies for improving the electrical transport property of vanadium and molybdenum oxide nanowire electrodes. Herein we presents some conventional and novel strategies such as doping [10-12], coating [13-15], prelithiation [16-18], and so on, to restrain the conductivity decrease of vanadium and molybdenum oxides as the electrodes of Li-ion batteries during the cycling processes by summarizing both the work done by other groups and the results of our own group.

2. Measurement of electrical transport

Electrical transport investigation is of great importance for fundamental research and technological applications in electrochemical energy storage. Although there are several methods of probing electrical properties of nanomaterials [19-28], there are two methods mostly used to measure the conductivity of nanomaterials. One is single nanowire device fabrication, and the other is directly measuring the films by 2 or 4 probes.

Single nanowire device for electrical measurement has been fabricated by some groups. The specific process of fabricating a device is described as follows as an example: the suspension of host nanowires in organic solvent (acetone, isopropanol, etc) is dispersed on SiO_2-coated Si wafer. Resist layers are spin-coated on the nanowires/wafer, and contact patterns are defined on the resist layers by e-beam lithography (EBL) or photolithography. The patterns are developed with corresponding solution. After these procedures, Au/Pd and other metals are evaporated on the resist,

J. Nanosci. Lett. 2012, **2**: 22
www.simplex-academic-publishers.com

1
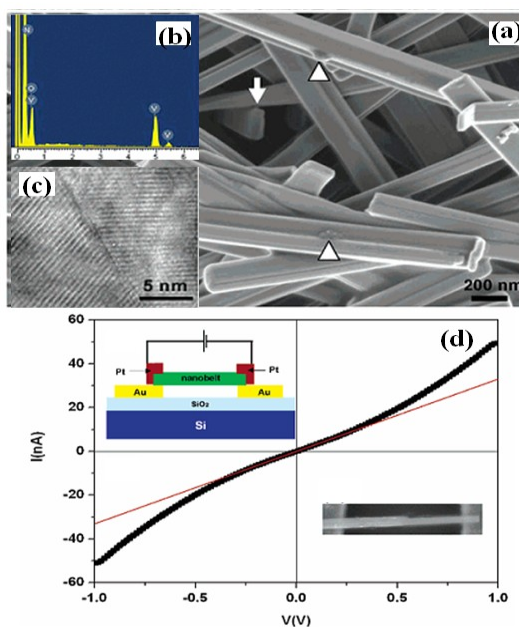
Figure 1. (a, b) Scanning electron microscope (SEM) image and energy dispersive spectroscopy (EDS) spectrum of $NH_4V_3O_8$ nanowire. (c) The representative high-resolution transmission electron microscope (HRTEM) image of the twin boundary present in a nanowire. (d) Current-voltage (I/V) curve of individual nanowire. Insets: the schematic view and the SEM image of the individual nanowire electrode, respectively [23].

and the final pattern formation is accomplished by lift-off in specific solution [21-22]. Based on this method, Mai et al. fabricated a single nanowire device of monoclinic $NH_4V_3O_8$ (illustrated Figure 1 inset) with widths of 80-180 nm, thicknesses of 50-100 nm, and lengths up to tens of micrometers [23]. They found the conductive mechanism is due to ohmic mechanism at low electric field below 249 V/cm, Schottky emission at medium electric field between 249 and 600 V/cm and the Poole–Frenkel emission mechanism at high field above 600 V/cm.

In 2010, Mai et al. designed and fabricated the smallest solid state electrochemical device with only one nanowire (Figure 2) [9]. In this device, there are no binders or conductive carbon additives introduced into the system, which contains just one nanowire as either cathode or anode and uses classical materials for counter electrode and electrolyte in this device. The design is very effective, as it can provide insights into the intrinsic
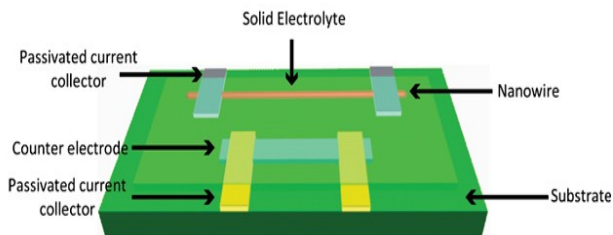
Figure 2. Schematic diagram of a single nanowire electrode device design [9].

reason for electrode capacity fading by combining single nanostructure transport study with electrode electrochemical performance test, without any other influencing factors.

Film measurement is also often employed to probe the electrical transport of nanomaterials. In the recent years, many groups prepared nanowires on the substrates to form nanowire thin films. In addition, the as-synthesized nanowire powder was dispersed in the solution and dropped on substrate to form nanowire thin film. The conductivity of the attained nanowire thin film is measured by semiconductor property analyzer. Chen et al. [23-25] investigated Mo-doped VO_2 nanowire array film, which was dip-coated on glass substrates from mixed MoO_3-V_2O_5 sol. The electrical property of Mo-doped VO_2 nanowire array film was measured by this means. It is very simple for this method to realize the measurement of conductivity, so it has been widely used to characterize transport property [26-28]. Notably, when the film gets thinner or is semiconducting, the conductance becomes lower and the two-point probe method need be used. But for traditional two-point probe method, the needle probe is put in contact with the sample through a very small area, and it is sometimes difficult to get enough conduction paths between the probes to detect the small current. In order to increase the electrical current, the point probes should be changed into line probes by drawing two lines of silver paste or other conductors on the sample surface for the landing of the point probes.

3. The optimization strategies

It is of necessity to point out that the conductivity decrease during cycling may be interrelated with structure degradation or phase transition of electrode materials. The other reasons for lowered conductivity may be the mixed phases acting as barriers to efficient electron conduction or changes in local electronic structure. So we will present different optimization strategies to overcome the conductivity decrease, based on different starting points.

3.1. Doping

Doping is an important method for enforcing and adjusting the properties of materials [26]. The introduction of the conductive metal ions to the host material is considered as an efficient mean to increase the electrical conductivity.

The electrical conductivity of pure V_2O_5 is very poor due to the $3d^0$ configuration of vanadium ions and a large energy gap between the conduction and the valence band (Eg~2.3eV) [29]. However, the electrical behavior of V_2O_5 is quite sensitive to the presence of the impurities [30]. So

doping could be an effective way to improve the conductivity of V_2O_5. In recent years, much work about doping layered oxides have been done by many research groups.

In 2006, Jiao et al. [31] reported that the electronic conductivity of $Cu_{0.1}$-doped VO_x-nanowires (NWs) was up to magnitude higher, comparing to undoped V_2O_5. They prepared $Cu_{0.1}$-doped VO_x-NWs by heating Cu-doped $V_2O_5 \cdot nH_2O$ gel (mix the selected stoichiometric amount of Cu powder with $V_2O_5 \cdot nH_2O$) under hydrothermal conditions in autoclave at 180 ^{o}C for 7 days. The research results also reveal that the doped vanadium oxide nanowires exhibit the improved kinetic behavior and rate capability. Yuan et al. [32] prepared $Cu_xV_2O_5$ by mixing Cu powder with V_2O_5 precipitate. The result showed that the Cu dopping increased the electronic conductivity of V_2O_5 without changing the layer structure of V_2O_5, leading to improvement of capacity and cycling performance.

Based on the work mentioned above, we come to the conclusion that the doping metallic ion into layered oxides could actually improve the conductivity. But the intrinsic reason and the fundamental mechanism remain unknown. Chen et al. [33] presented us an acceptable explanation. They made different amount of peroxo-polymolybdate solution mixed with V_2O_5 sol to form a mixed sol, then kept it into autoclaves at 180 ^{o}C for 12 h. The films were deposited onto indium tin oxides (ITO) conducting glass substrates by the dip-coating technique using the Mo-doped V_2O_5 sols. By SEM observation, it was found for film thickness to be about 800 nm for Mo-doped V_2O_5 film. An explanation is given that Mo-doped V_2O_5 creates energy levels in the band gap of V_2O_5, accompanying with the reduction of the forbidden-band width and the increase of the conductivity which leads to the enhancement of the electrochemical and electrochromic properties of the films.

Similarly, due to its special layered structural characteristics, molybdenum oxide (MoO_x) is also one of the most attractive metal oxides. However, molybdenum oxides have a low conductivity that largely limits its electrochemical performance. Many researchers tried their best to find effective ways to get conductivity enhanced. Elaidio et al. [34] used a wet chemistry method to prepare a new phase $Bi_{10}Mo_3O_{24}$ with $Bi(NO_3)_3 \cdot 5H_2O$ and MoO_3 as precursor at low temperature, and then investigated the relationships between the structure and conductivity. A preliminary heavy-atom skeleton related to the fluorite structure allowed us to postulate a layer structure with composition $[Bi_{10}O_{12}]_n[MoO_4]_{3n}$, exhibiting better ionic conductive properties in the whole temperature range. They provided two potential oxygen diffusion pathways, in the columnar and layer structure types of phases of the Bi_2O_3-MoO_3 system respectively.

Obviously, similar layered structure formed by MoO_4 packing favors a good conductivity.

Muralidharan et al. [27] studied the structural and electrochromic properties of pure and cerium doped molybdenum oxide films. Cerium (5–15% by weight) doped molybdenum oxide thin films were prepared on FTO coated glass substrate at 250 ^{o}C using sol–gel dip coating method. By measuring the capacitance performance and cycling stability, it was found that cerium doped thin films exhibited high oxygen ion conductivity. The pure molybdenum oxide films exhibit an anodic current density of 1.90 mA/cm^2 at 25th cycle and 0.65 mA/cm^2 at 60th cycle, where for the cerium doped molybdenum oxide films it was 2.80 mA/cm^2 at 25th cycle and 1.37 mA/cm^2 at 130th cycle. This study clearly indicates that cerium doping enhances the electrochromic performance and stability of molybdenum oxide films.

3.2. Coating

Coating layer often acts as an elastic buffer to relieve the strain associated with volume variations during lithium insertion/extraction reaction. Based on this point, it can be concluded that coating another kind of material on the surface of the host material is an effective way to make structure more stable. Therefore, if conductive materials, such as carbon and conducting polymers (polypyrrole (PPy), polyaniline (PANI), poly (3, 4-ethylenedioxy thiophene) (PEDT), etc.) [35-39], were used as the coatings, the defect of low-conductivity of the electrode materials could be solved to some extent. In addition, the flexibility of carbon and conducting polymers could facilitate the electron transport and ion diffusion into the core materials.

As we know, PANI has unique characteristic compared with other conducting polymers, which can realize rapidly conversion between the base (insulator) and the salt form (conductor) by treatment with acid or electrochemical means. PANI also has good environmental stability and high electrical conductivity [40], which make it play an important role in preparing complex structure nanowires.

Much work has been done to prepare nanowires by adding PANI which have improved the conductivity of host materials and obtained appropriate electrochemical performance to some extent. In 2009, Kulkarn et al. [41] synthesized PANI/V_2O_5 by adopting microwave-assisted hydrothermal method. The conductivity of the PANI/V_2O_5 nanowires was measured by standard two probe conductivity measurement technique. The room temperature conductivity was found to be 2.27×10^{-5} S/cm. Ruckenstein et al. [42] conducted further work about PANI/V_2O_5. The nanowires with an ordered mesostructure were obtained. Its electrical conductivity was about 10^{-2} S/cm, which was higher than the as-prepared V_2O_5 mesostructured phase (10^{-7} S/cm) by 5 orders of magnitude.
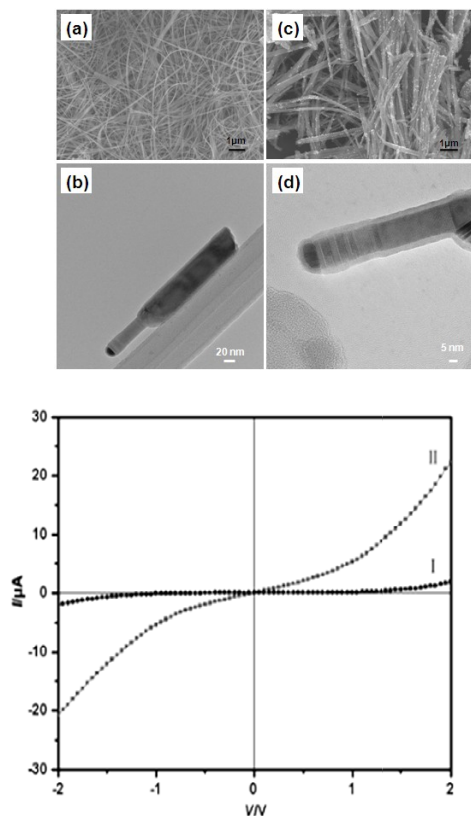
Figure 3. (a, b) Typical FE-SEM and TEM images of β-AgVO$_3$ nanowires. (c, d) Typical FE-SEM and TEM images of AgVO$_3$/PPy nanocables. (e) I-V curves of β-AgVO$_3$ nanowires (I) and AgVO$_3$/PPy nanocables(II).

Polyaniline is also used to improve the electrochemical property of molybdenum oxide. In 2009, Pan et al. [43] prepared MoO$_3$/PANI nanowires by ion-exchange reaction between aniline (ANI) and dodecylamine (DDA). According to the results of the ohmic resistance of MoO$_3$/PANI electrode, its ohmic resistance is less than that of pure MoO$_3$ electrode, which indicates that the electrical conductivity of MoO$_3$ is increased by intercalating PANI into this composite. In the same year, Prasad et al. [44] synthesized MoO$_3$/PANI by chemical oxidation method and got the similar result of conductivity increasing. Based on the results mentioned above, a conclusion can be obtained that PANI can effectively improve the conductivity of layered vanadium and molybdenum oxides.

Meanwhile, other conductive polymers, due to their high stability such as PPy, also attracted a lot of attention to modify electrochemical performance of nanowires. Our group has devoted ourselves to constructing AgVO$_3$/PPy coaxial nanocable. AgVO$_3$/PPy coaxial nanocable can be obtained by the redox reaction between β-AgVO$_3$ and pyrrole monomer in the presence of perchloric acid, in which β-AgVO$_3$ was prepared by the hydrothermal method. [45]. According to the SEM image (Figure 3c), AgVO$_3$/PPy coaxial nanocable had the rougher

surface and the increased diameter, on the basis of retainment of the one-dimensional morphology. The detailed morphology information was further confirmed by TEM results. AgVO$_3$/PPy coaxial nanocables exhibit the core/shell structure (Figure 3d). That is to say, PPy uniformly coated on the surface of β-AgVO$_3$ nanowires, and it was found that the thickness of covering layer was around 6 nm. AgVO$_3$/PPy coaxial nanocables were used as the cathode active materials to assemble Li-ion batteries, which showed that they exhibited better electrochemical cycling stability than the original nanowires. In order to further characterize the electric transport properties of AgVO$_3$/PPy coaxial nanocable, a nanowire device was designated to test its I-V property by 2-probe method in the air with voltage scanning range of -2~2V (shown as Figure 3e). The materials dispersed on the silicon substrate and silver electrodes were plated on the both ends of the film. From the image we discovered that the β-AgVO$_3$ nanowires and AgVO$_3$/PPy coaxial nanocable both presented symmetrical nonlinear curves, but the peak point current of PPy coating nanowires is much larger than that of the original nanowires. According to the conductivity calculation formula, the conductivity of β-AgVO$_3$ nanowires is estimated at 1.5×10^{-4} S/cm, while the AgVO$_3$/PPy coaxial nanocable presents that about 1.3×10^{-3} S/cm, which is an order of magnitude higher than the original one. From the comparison above, we can conclude that constructing coaxial nanocable with conductive polymer can achieve high conductivity which is favorable for the cathode materials.

Carbon coating is another method to increase conductivity. In 2009, C/MoO$_3$ was synthesized by a simple hydrothermal route by Hassan et al [46]. In the electrochemical results, the C/MoO$_3$ nanowires exhibit excellent cycling stability with a current rate of 0.1C, maintaining their capacity at 1064 mAh g^{-1} after 50 cycles which are better than those of bare MoO$_3$ nanowires electrode. The excellent electrochemical performance of the C/MoO$_3$ nanowires are attributed to the effects of the carbon coating which stabilizes the structure of the MoO$_3$, enhances the ionic/electrical conductivity, and can serve as a buffering agent to absorb the volume expansion during the Li$^+$ intercalation process.

From all mentioned above, polymer and carbon coating are effective to increase the conductivity as well as the structure stability of layered oxide.

In addition to polymer and carbon coating, there still exist some other coating methods, such as metallic oxide. In 2005, Li et al. [47] used mild hydrothermal reaction to prepare vanadium oxides nanowires coated with Fe$_2$O$_3$, TiO$_2$ and SnO$_2$ nanoparticles. Nakayama et al. [48] deposited manganese and molybdenum mixed oxides on a platinum substrate to form a thin film and tested the electrode at potential between 0 and 1.0 V vs

4
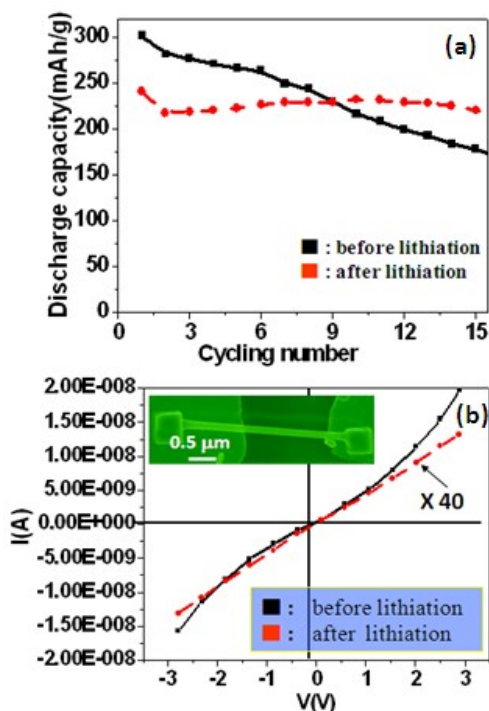
Figure 4. (a) The discharge capacity as a function of the cycle number for the MoO_3 nanowires before and after lithiation. (b) I/V transport measurements of single nanowire fabricated devices using the samples before and after lithiation [16].

Ag/AgCl in aqueous manganese(II) solutions containing molybdate anion (MoO_4^{2-}). As they expected, the electrical conductivity of the film increased.

3.3. Prelithiation

Prelithiation is considered as an effective way to increase the cycling stability of cathode and/or anode materials as well as to investigate the structural changes of the electrode materials during lithium ion insertion [18]. Compared with pristine materials, the prelithiated samples not only keep their original structure, but also get the conductivity increased.

Taking Li_yVO_x one dimensional structure for example, many researchers found that they presented the improved electrochemical performance because of their special one dimensional structure and the incorporation of lithium-ions into the host lattice by strong ionic bonds, which can improve the structural stability and electronic conductivity of the cathode materials [49-51]. EIS results indicated the distinctly higher electronic conductivity of Li_yVO_x-NWs than that of VO_x-NWs. As a result, Li_yVO_x-NWs exhibit high discharge capacity and good cycling performance compared to VO_x-NWs, due to the fact that the presence of more vacant sites for Li^+-ions [52].

Recently, Mai et al. has investigated prelithiation of MoO_3 nanowire. They [16] assembled

a single nanowire device to measure the electrical transport through an individual MoO_3 nanowire before and after lithiation. As shown in Figure 4a, the cycling performance can be improved by secondary hydrothermal lithiation. To understand the enhanced performance of lithiated nanowires for Li^+ storage, they measured the electrical transport through individual MoO_3 nanowires before and after lithiation (Figure 4b). A single nanowire was placed across two gold electrodes, and the final contacts were improved by Pt deposition at the two ends. Before lithiation, the I/V characteristics of the nanowire shows asymmetric Schottky barriers at the two ends (the solid curve in Figure 4b), created between semiconductor MoO_3 and Au/Pt electrode, and the transported current is in the order of ca. 300 pA at ca. 2 V. After lithiation, the I/V curve shows ohmic behavior (the dashed curve in Figure 4b), and the transported current is of the order of 10 nA at a bias of ca. 2 V. Using the measured resistance, the effective length, and cross section of the nanowire, the conductivity is evaluated to be approximately 10^{-4} Scm^{-1} and 10^{-2} Scm^{-1} before and after lithiation, respectively, which increases by close to two orders of magnitudes. The improvement of the cycling performance for the lithiated sample (Figure 4a) may be attributed to the enhanced structural stability of the electrodes as a result of lithiation, which possibly indicates a reduced volumetric change of the nanowire electrode. The Li^+ ions, first introduced during lithiation and later remained in the lattice, enhance the electrical conductivity, which may assist the transport of the Li^+ ions to be inserted and extracted in future charge–discharge processes.

3.4. Other strategies

In addition to those we mentioned above, there are some other methods of modification, for instance orientation growth and porous technology, etc. Ordered nanowire architectures, compared with nanowires with disordered form, have bigger specific surface area and lower average concentration of structural defects and grain boundaries, resulting in increased Li^+ insertion/extraction rate and electron transport.

Mai et al. conducted the work on VO_2 orientation assembly via the Langmuir-Blodgett (LB) technique which can readily help to assemble one-dimensional nanostructures into large-area ordered monolayer arrays at the air-water interface. The chloroform VO_2 nanowire suspension was spread dropwise on the aqueous phase of a LB trough to assemble VO_2 nanowire film [53]. The inset of Figure 5 shows typical SEM images of VO_2 nanowire LB films deposited at surface pressure of 40 mN/m, in which ordered VO_2 nanowire in local area can be seen. They carried out X-ray diffraction (XRD) analysis of the transferred films of VO_2 nanowires functionalized by stearic acid (SA) and cetyltrimethylammonium bromide (CTAB) to probe for additional structural order. Notably, the typical
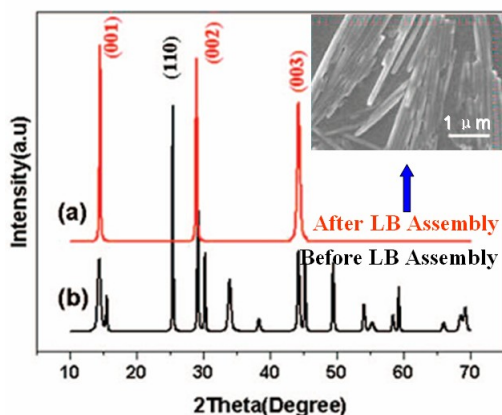
Figure 5. The X-ray diffraction (XRD) patterns of VO$_2$ nanowire LB films (a) and as-synthesized VO$_2$ nanowires without LB assembly (b). The inset is the SEM image of VO$_2$ nanowire LB films [53].

XRD pattern of VO$_2$ nanowire LB films (Figure 5a) only exhibits (001) peaks, while diffraction peaks characteristic of other crystalline planes are absent. These observations contrast XRD analysis of VO$_2$ nanowires transferred to the same substrates without LB assembly process (Figure 5b). Hence, we can conclude that the VO$_2$ nanowires in LB film have a well-defined (00*l*) crystal plane orientation. Moreover, to confirm the influence of orientation growth on the performance of VO$_2$ nanowires, the cyclic voltammetry (CV) and I/V were investigated. According to the results, we know that there is an obvious improvement in electrochemical capacity by 2 orders and the conductivity also increases apparently.

Electrodeposition method was used to grow non-stoichiometric mixed-valent molybdenum (VI,V) oxide film on carbon substrates by Dong et al. [54]. The results show that the characteristic domed structure on the film surface was enlarged during the state transition from the oxidized to the reduced with no significant change in the Root Mean Square (RMS) surface roughness value. Meanwhile, based on many investigations, a point was demonstrated that the redox activity and conductivity of the oxide film depend largely on the extent of hydration and porosity. As in the hydration process, many of the coordinated oxygen species (OH or OH$_2$) are terminal, which results in the more open structure of these materials. Also, electrons are introduced into the film during the reductive steps; this dispersion allows protons (H$_3$O$^+$) to enter the film easily to equilibrate the charge, which results in a more porous structure with good conductivity [55-57].

4. Conclusions and outlook

In this review, taking layer vanadium oxide and molybdenum oxides for examples, we present some strategies to restrain the conductivity decrease, such as doping, coating, prelithiation, and so on.

Besides these strategies which researchers have put forward, some other potential approaches to improve the electrochemical performance of Li-ion battery remain to be seen, such as combining these strategies to realize their synergistic effect, functional structure construction, or essentially developing new LIB electrode materials and new synthetic techniques. As we know Li-ion battery is one of green energy devices, and its development means benefitting human and environment more. Looking forward, due to the fact that a great variety of optimizing strategies can overcome these problems in Li-ion battery, such as capacity fading etc, it will be widely used in various fields, and the future appears remarkably bright.

References

1. N.A. Chernova, M. Roppolo, A.C. Dillon and M.S. Whittingham, J. Mater. Chem. 19 (2009) 2526.
2. M.S. Whittingham, Chem. Rev. 104 (2004) 4271.
3. Y.Y. Qi, W.Chen, L.Q. Mai, Q.Y. Zhu, A.P. Jin, Int. J. Electrochem. Sci. 1 (2006) 317.
4. L. F. Nazar, B. E. Koene, and J. F. Britten, Chem. Mater. 8 (1996) 327.
5. W. Chen, L.Q. Mai, Y.Y. Qi and Y. Dai, J. Phys. Chem. Solids 67 (2006) 896.
6. C. Ban, N.A. Chernova, and M.S. Whittingham, Electrochem. Commun. 11 (2009) 522.
7. L.Q. Mai, W. Chen, Q. Xu, J.F. Peng, Q.Y. Zhu, Chem. Phys. Lett. 382 (2003) 307.
8. L.Q. Mai, W. Chen, Q. Xu, and Q.Y. Zhu, Microelectron. Eng. 66 (2003) 199.
9. L.Q. Mai, Y.J. Dong, L. Xu, and C.H. Han, Nano Lett. 10 (2010) 4273.
10. Y.J. Lee, M.G. Kim, and J. Cho, Nano Lett. 8 (2008) 957.
11. E.M. Sorensen, H.K. Izumi, J.T. Vaughey, C.L. Stern, and K. R. Poeppelmeier, J. Am. Chem. Soc. 127 (2005) 6347.
12. N.Y. Shishkin, A.A. Komarov, D.V. Kosov, V.A. Cherkasov, L.A. Bashkirov, U. Bardi, and Y.K. Gunko, Sensor. Actuat. B 108 (2005) 113.
13. X.H. Xia, J.P. Tu , J. Zhang, X.H. Huang, X.L. Wang, W.K. Zhang and H. Huang, Electrochem. Commun. 10 (2008) 1815.

6

J. Nanosci. Lett. 2012, **2**: 22
www.simplex-academic-publishers.com

14. X.H. Huang, J.P. Tu, X.H. Xia, X.L. Wang, and J.Y. Xiang, Electrochem. Commun. 10 (2008) 1288.

15. S.R. Gowda, A.L.M. Reddy, M.M. Shaijumon, X.B. Zhan, L.J. Ci, and P.M. Ajayan, Nano Lett. 11 (2011) 101.

16. L.Q. Mai, B. Hu, W. Chen, Y.Y. Qi, C.S. Lao, R.S. Yang, Y. Dai, and Z.L. Wang, Adv. Mater. 19 (2007) 3712.

17. L.Q. Mai, B. Hu, Y.Y. Qi, Y. Dai, and W. Chen, Int. J. Electrochem. Sci. 3 (2008) 216.

18. L.Q. Mai, L. Xu, B. Hu, and Y.H. Gu, J. Mater. Res. 25 (2010) 1413.

19. H.J. Dai, E. W. Wong, and C.M. Lieber, Science 272 (1996) 523.

20. S. Furusawa, T. Kasahara, A. Kamiyama, Solid State Ionics 180 (2009) 649.

21. J.Y. Li, L. An, C.G. Lu, and J. Liu, Nano Lett. 6 (2006) 148.

22. H. Ruda, J. Salfi, U. Philipose, A. Saxena, K.T. Lau, T. Xu, L. Zhong, C.D. Souza, S, Aouba, S.X. Yang, P. Sun, S. Nair, and C. Fernandes, J. Mater. Sci: Mater. Electron. 20 (2009) S480.

23. L.Q. Mai, C.S. Lao, B. Hu, J. Zhou, Y.Y. Qi, W. Chen, E.D. Gu, and Z.L. Wang, J. Phys. Chem. B 110 (2006) 18138.

24. L.Q. Mai, W. Chen , Q. Xu, J.F. Peng, and Q.Y. Zhu, Chem. Phys. Lett. 382 (2003) 307.

25. L.Q. Mai, W.L. Guo, B. Hu, W. Jin, and W. Chen, J. Phys. Chem. C 112 (2008) 423.

26. B. Chen, D.F. Yang, Paul A. Charpentier, and M. Zeman, Sol. Energ. Mat. Sol. C. 93 (2009) 1550.

27. M. Dhanasankar, K.K. Purushothaman, and G. Muralidharan, Mater. Res. Bull. 45 (2010) 1969.

28. Z.F. Luo, Z.M. Wu, X.D. Xu, M.J. Du, T. Wang, and Y.D. Jiang, Mater. Sci. Eng. B 176 (2011) 762.

29. A. Chakrabarti, K. Hermann, R. Druzinic, M. Witko, F. Wagner, and M. Petersen, Phys. Rev. B. 59 (1999) 10583.

30. J.H. Perlstein, J. Solid State Chem. 3 (1971) 217.

31. H.X. Li, L.F. Jiao, H.T. Yuan, M. Zhao, M. Zhang, and Y.M. Wang, Mater. Lett. 61 (2007) 101.

32. L.F. Jiao, H.T. Yuan, Y.C. Si, Y.J. Wang, and Y.M. Wang, Electrochem. Commun. 8 (2006) 1041.

33. A.P. Jin, W. Chen, Q.Y. Zhu, Y. Yang, V.L. Volkov, and G.S. Zakharova, Thin Solid Films 517 (2009) 2023.

34. E. Vila, J.E. Iglesias , J. Galy, and A. Castro, Solid State Sci. 7 (2005) 1369.

35. S. Kuwabata, S. Masui, and H. Yoneyama, Electrochim. Acta 44 (1999) 4593.

36. R. Liu, and S.B. Lee, J. Am. Chem. Soc. 130 (2008) 2942.

37. A.P. Jin, W. Chen, Q.Y. Zhu , Y. Yang, V.L. Volkov , and G.S. Zakharova, Solid State Ionics 179 (2008) 1256.

38. P.O. Herenilton, F.O.G. Carlos, A.B. Carlos, and M.G. Elídia, J. Non-Cryst. Solids 273 (2000) 193.

39. Y.J. Liu, J.L. Schindler, D.C. Degroot, C.R. Kannewurf, W. Hirpo, and M.G. Kanatzidis, Chem. Mater. 8 (1996) 525.

40. I. Karatchevtseva, Z. Zhang, J. Hanna, and V. Luca, Chem. Mater. 18 (2006) 4908.

41. M.A. Jagtap, M.V. Kulkarni, S. K. Apte, S.D. Naik, and B.B. Kale, Mater. Sci. Eng. B 168 (2010) 199.

42. Z.F. Li and E. Ruckenstein, Langmuir 18 (2002) 6956.

43. A.Q. Pana, D.W. Liu, X.Y. Zhou, B.B. Garcia, S.Q. Liang, J. Liu, and G.Z. Cao, J. Power Sources 195 (2010) 3893.

44. Koppalkar R. Anilkumar, Ameena Parveen, G.R. Badiger, and M.V.N. Ambika Prasad, Physica B 404 (2009) 1664.

45. L.Q. Mai, L. Xu, Q. Gao, C.H. Han, B. Hu, and Y.Q Pi, Nano Lett. 10 (2010) 2604.

46. M.F. Hassan, Z.P. Guo, Z. Chen, and H.K. Liu, J. Power Sources 195 (2010) 2372.

47. J.F. Liu, X. Wang, Q. Peng, and Y.D. Li, Sensor. Actuat. B 115 (2006) 481.

48. M. Nakayama, A. Tanaka, Y. Sato, T. Tonosaki, and K. Ogura, Langmuir 21 (2005) 5907.

49. C.J. Cui, G.M. Wu, J. Shen, B. Zhou, Z.H. Zhang, H.Y. Yang, and S.F. She, Electrochim. Acta 55 (2010) 2536.

50. L. Liu, L. Jiao, J. Sun, Y. Zhang, M. Zhao, H. Yuan, and Y. Wang, J. Alloy. Compd 471 (2009) 352.

51. L. Liu, L. Jiao, J. Sun, M. Zhao, Y. Zhang, H. Yuan, and Y. Wang, Solid State Ionics 178 (2008) 1756.

52. M.S. Bhuvaneswari, S. Selvasekarapandian, S. Fujihara, and S. Koji, Solid State Ionics 177 (2006) 121.

53. L.Q. Mai, Y.H. Gu, C.H. Han, B. Hu, W. Chen, P.C. Zhang, L. Xu, W.L. Guo, and Y. Dai, Nano Lett. 9 (2009) 826.

54. S.Q. Liu, Q.B. Zhang, E. Wang, and S.J. Dong, Electrochem. Commun. 1 (1999) 365.

55. P.J. Kulesza, and L.R. Faulkner, J. Am. Chem. Soc. 110 (1988) 4905.

56. L.D. Burke, and E.J.M. O'Sullivan, J. Electroanal. Chem. 117 (1980) 155.

57. L.D. Burke, T.A.M. Twomey, and D.P. Whelan, J. Electroanal. Chem. 107 (1980) 201.

J. Nanosci. Lett. 2012, **2**: 22
www.simplex-academic-publishers.com

7

8

J. Nanosci. Lett. 2012, **2**: 22
www.simplex-academic-publishers.com